# Use of two-dimensional photoelectron spectroscopy in the decomposition of an inner-shell excitation spectrum broadened by super-Coster-Kronig decay

A. Kivimäki,[1,*] P. Norman,[2] M. Coreno,[3] M. de Simone,[1] C. Grazioli,[4] R. Totani,[5] B. Ressel,[6] H. Ottosson,[7] and C. Puglia[8]

[1]*Consiglio Nazionale delle Ricerche - Istituto Officina dei Materiali, Laboratorio TASC, 34149 Trieste, Italy*

[2]*Department of Physics, Chemistry and Biology, Linköping University, 581 83 Linköping, Sweden*

[3]*Consiglio Nazionale delle Ricerche, Istituto di Metodologie Inorganiche e dei Plasmi, Via Salaria km 29.300,*
*00019 Monterotondo Scalo, Rome, Italy*

[4]*Elettra-Sincrotrone Trieste, Area Science Park, 34149 Trieste, Italy*

[5]*Dipartimento di Scienze Fisiche e Chimiche, Universitá degli Studi dell' Aquila, 67100 L' Aquila, Italy*

[6]*Laboratory of Quantum Optics, University of Nova Gorica, 5270 Ajdovščina, Slovenia*

[7]*Department of Chemistry - BMC, Uppsala University, Box 576, 751 23 Uppsala, Sweden*

[8]*Department of Physics and Astronomy, Uppsala University, Box 516, 751 20 Uppsala, Sweden*

(Received 26 July 2013; published 2 December 2013)

The Ge $3p$ core excitation spectrum of the $n$-butylgermane molecule only reveals two peaks, whereas the rest of the fine structure is obscured due to the large lifetime broadenings of core-excited states. A two-dimensional presentation of resonant photoemission spectra allows us to observe some other resonances. The interpretation of experimental results is supported by *ab initio* calculations conducted at the four-component relativistic level of theory with full account made for spin-orbit interactions already in the zeroth-order Hamiltonian.

## I. INTRODUCTION

Observed widths in inner-shell photoelectron and excitation spectra become extremely wide, if the core hole state in question can decay via Coster-Kronig (CK) or super-Coster-Kronig (sCK) transitions. These transitions have very high probabilities, which increase the inherent lifetime widths of core hole states. In CK and sCK transitions, one and two final state holes, respectively, are located in the same shell as the initial state hole. As an example of their effect on the lifetime widths, the Ar $2s^{-1}$ state can decay via $2s^{-1} \rightarrow 2p^{-1}3s^{-1}$ and $2s^{-1} \rightarrow 2p^{-1}3p^{-1}$ CK transitions and its lifetime width is $2.25 \pm 0.05$ eV [1]. In contrast, the core-ionized $2p^{-1}$ states of Ar decay via $L_{2,3}MM$ Auger transitions, which results in a much smaller lifetime widths of $118 \pm 4$ meV [2]. The lifetime widths of core-excited states are typically similar to the analogous core-ionized states [2]. Consequently, the Ar $2p$ core excitation spectrum is well resolved [3], whereas different excitations strongly overlap in the Ar $2s$ spectrum [4]. The latter is, in principle, understood because it can only be composed of Ar $2s \rightarrow np$ ($n \geqslant 4$) Rydberg excitations, whose energies can be estimated rather accurately or calculated using quantum mechanical codes. The situation may be much more complicated in molecules. In general, molecular core excitation spectra show transitions to both valence and Rydberg orbitals, and each electronic transition is typically accompanied by the excitation of vibrational modes. Therefore core excitation spectra of molecules can become intractable if core-excited states de-excite via CK or sCK transitions.

The lifetime width of a core-excited state can be overcome in electronic decay spectra due to the so-called Auger resonant Raman effect, if a narrow photon band (narrower than the lifetime width) is used to excite an inner-shell electron to an unoccupied orbital [5]. One might then consider that if the peak structure of the decay spectrum is simple enough, its resolution-enhanced changes as a function of photon energy could carry telltale signs of different core-excited states even when those states are not resolved in the x-ray absorption spectrum. The $3p$ core-hole states of germanium are known to decay via sCK transitions in atoms, molecules, and solids [6–8]. In the present paper we have investigated the Ge $3p$ inner-shell absorption of the $n$-butylgermane (NBG, $CH_3CH_2CH_2CH_2GeH_3$) molecule by measuring its resonant sCK decay spectra. The NBG molecule has recently attracted interest because it is a candidate precursor for growing Ge nanowires that have potential applications in diverse areas such as sensors and energy storage [9].

In our series of measurements both the photon energy step and the bandwidth of incident photons were considerably smaller than the lifetime width of the core-excited states (about 2 eV). Representation of the two-dimensional spectra as contour plots then reveals some resonances that are not observed in the ordinary core excitation spectrum. This way of performing measurements has been called two-dimensional photoelectron spectroscopy (2DPES) [10] and it has been used earlier in core level studies of atoms and molecules. For instance, Odling-Smee *et al.* [11] exploited 2DPES to study post-collision interaction just above the Br($3d$) edge of the HBr molecule, whereas both Kukk *et al.* [12] and Sokell *et al.* [13] used it to illustrate different resonant Auger decay channels—including decay in core-excited Cl atoms following ultrafast dissociation—after the excitation of the Cl $2p$ electrons to unoccupied orbitals in the HCl molecule. A more recent application has been the observation of the $1s \rightarrow 2p$ resonance in singly ionized neon, achieved using highly brilliant ultrashort x-ray pulses from a free-electron laser source [14]. A closely related method to 2DPES is constant ionic state (CIS) spectroscopy: An electron spectrometer registers counts in a fixed binding energy window, corresponding to a chosen final ionic state, when photon

___
*Corresponding author: kivimaki@iom.cnr.it

energy is scanned across the excitation region of interest. A CIS spectrum can actually be obtained from two-dimensional photoelectron spectra by cutting a slice in the appropriate direction [10]. CIS spectroscopy can be used to decompose an absorption spectrum, as has been demonstrated, e.g., for the $3p$ excitations in Cu atoms [15] and for the N $1s \rightarrow 2\pi$ excitations in the NO molecule [16].

## II. EXPERIMENT

The experiments were carried out at the Gas Phase Photoemission beamline [17] at the Elettra synchrotron radiation laboratory in Trieste, Italy. Undulator radiation in the photon range of 14–900 eV is monochromatized by a spherical grating monochromator, equipped with a planar premirror and five interchangeable gratings. Electron spectra were measured using the original SES-200 electron analyzer [18], mounted at the magic angle (54.7 deg) with respect to the electric vector of the linearly polarized incident light. The use of this angle allows one to record angle-integrated electron spectra. The pass energies of 50 and 100 eV were used in the measurements, yielding the kinetic energy resolution of about 0.11 and 0.22 eV, respectively. The kinetic energy scale of the electron analyzer was calibrated against the $N_{4,5}OO$ Auger lines of xenon [19]. The photon energy scale was subsequently calibrated by recording the Xe $4d$ photoelectron lines, whose binding energies are accurately known [3]. The Ge $3p$ core excitation spectrum was measured with the total ion yield method using a microsphere plate detector in the current mode. The photon flux was measured simultaneously with a calibrated Si photodiode for normalization purposes. The NBG sample, which is liquid at room temperature, was acquired from ABCR GmbH & Co., KG, Germany, with a stated purity of 95%. It was further purified through freeze-pump-thaw cycles until no bubbles were seen upon melting. Sample molecules were let into the interaction region through a hypodermic needle. The pressure in the experimental chamber was set at $5 \times 10^{-6}$ mbar, but the local pressure just above the needle is estimated to be 10–50 times higher.

## III. COMPUTATIONAL DETAILS

The electronic structure of NBG was studied at the four-component relativistic level of theory, employing the Dirac-Coulomb Hamiltonian as implemented in the Dirac program [20]. Spin-own-orbit interactions were thus fully accounted for in the zeroth-order Hamiltonian and included in the energies of the orbitals forming doubly occupied Kramers pairs as a consequence of time-reversal symmetry.

Our theoretical estimates for ionization potentials (IPs) are based on the $\Delta$SCF approach. In situations of orbital degeneracy, or near degeneracy, we optimize the ionic state by means of the average-of-configuration technique, specifying occupation of a certain number of electrons in a certain number of degenerate, or near degenerate, orbitals. We choose to consider the $3p_{1/2}$ and $3p_{3/2}$ shells in separate calculations with specifications for the electronic structures of the ions as 1 electron in 2 orbitals (1-in-2) and 3-in-4, respectively.

Absorption in the near-edge spectral region is described with the relativistic static-exchange (STEX) approach [21], in which oscillator strengths are obtained in the electric-dipole approximation by forming the transition moments between the Hartree-Fock ground state and the configuration interaction singles (CIS) description of the core-excited states. The method has been applied to the study the $L$ edges of sulfur and silicon, in applications of gold surface absorption [22,23].

NBG was optimized in $C_s$ symmetry at the level of density functional theory (DFT) in conjunction with the hybrid B3LYP [24] exchange correlation functional and the all-electron cc-pVDZ [25] basis set, which corresponds to a Ge–C bond distance of 1.981 Å. For the property calculations, we employ basis sets t-aug-cc-pVTZ for germanium and aug-cc-pVDZ for carbon and hydrogen. These basis sets are used for the description of the large components of the spinors and the condition of restricted kinetic balance is employed for the formation of basis sets for the corresponding small components. Two-electron integrals of the type small–small are not included in the calculation, an approximation that is expected to be highly accurate in the present case [26].

The ground state of NBG is closed shell in nature and the electronic configuration refers to the double occupation of four-component Kramers pair orbitals that couple to one another by means of the time-reversal operator; in the nonrelativistic limit this corresponds to a double occupation of $\alpha$- and $\beta$-spin orbitals. A characteristic of the STEX method with its explicit treatment of electronic relaxation (and thus electron correlation) is that the final multielectron state in the absorption process can be written as a very compact determinant expansion involving, for a given transition, only a single or a few of the virtual (virt) orbitals of the core ionized reference state. So the electronic configuration is in this case occupied$^{-1}$virt$^1$. In an expansion using the ground state orbitals, this would not be true and the excited state wave function would refer to a lengthy determinant expansion without a clear electronic configuration; electron correlation would need to be taken into account by the wave function expansion. In the discussion below we have detailed to what extent a final multielectron wave function is characterized by a single-particle excitation but we have omitted detailed orbital characterizations (such as isoelectron density plots) as we feel they would not contribute any added value to the overall purpose of the article (which is to demonstrate the experimentally increased resolution of excited states).

## IV. EXPERIMENTAL AND THEORETICAL RESULTS

The experimental Ge $3p_{3/2}$ and $3p_{1/2}$ ionization energies of NBG were determined to be $128.9 \pm 0.2$ and $133.1 \pm 0.2$ eV, respectively, whereas the corresponding theoretical results are equal to 132.0 and 135.9 eV. The spin-orbit splitting is thus well accounted for but the theoretical results suffer from an overall shift due effects of electron correlation. Figure 1(a) shows the Ge $3p$ excitation spectrum of NBG, measured using the total ion yield method, after normalization to the photon flux and subtraction of a linear background. Only two peaks can be discerned with certainty in the experimental data. A Lorentzian fit gave the FWHM (full width at half maximum) of 2.0 eV for the most intense core excitation (several peaks were included in the high-energy part of the spectrum in order to get a realistic fit). As the photon energy resolution (about
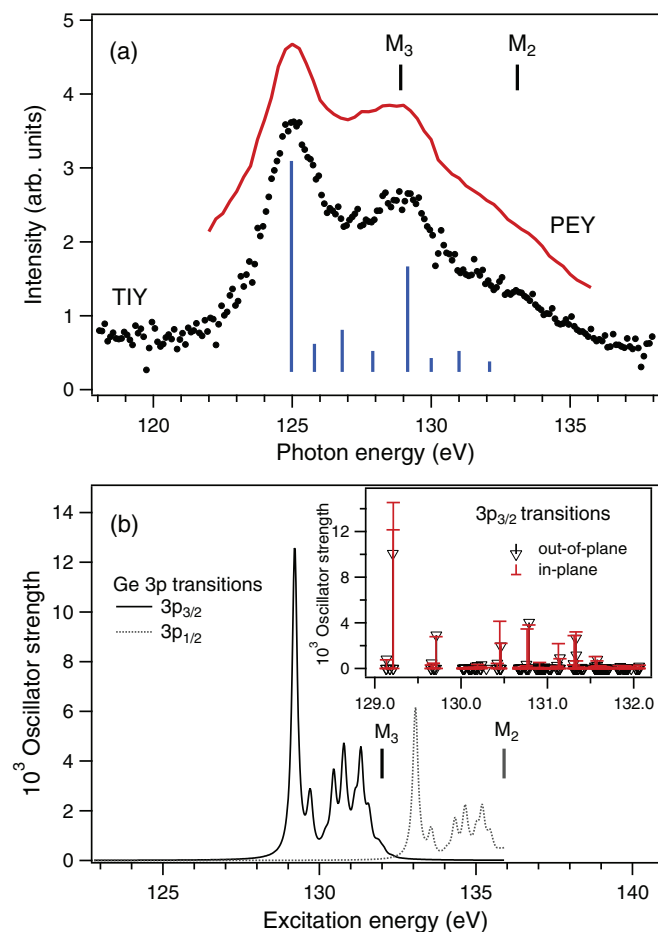
FIG. 1. (Color online) The normalized and background-subtracted total ion yield (TIY) spectrum of NBG at the Ge $3p$ edge. The solid curve shows the background-subtracted partial electron yield (PEY) in the binding energy range of 30–100 eV. Bars under the TIY curve indicate the positions of core excitations found in this work. (b) The calculated Ge $3p_{3/2}$ and $3p_{1/2}$ x-ray absorption spectra of NBG after convolution with a 0.2 eV FWHM Lorentzian broadening. The insert shows out-of-plane and in-plane transitions for Ge $3p_{3/2}$ excitations.

70 meV) was negligible in comparison, our estimate for the lifetime broadening of the core-excited state is also 2.0 eV. The energies of the two most intense excitations were determined to be 124.91 ($\pm 0.10$) and 129.10 ($\pm 0.15$) eV. Their difference of 4.19 eV agrees very well with the spin-orbit splitting of 4.2 eV found in the Ge $3p$ photoelectron spectrum.

The Ge $3p$ pre-edge region was calculated with the STEX approach. Since the reference states for CIS calculations are based on the respective ionic orbitals, there is a direct account for the electronic relaxation effects in the excited states but there is no account made for polarization effects. By polarization effects here we refer to interactions between the excited core electron and surrounding valence electrons. The lack of polarization in the reference state determinant inflicts a small compression of the pre-edge regions. The $M_2$ and $M_3$ pre-edge regions are predicted to be about 3 eV wide at this level of theory. Since, in the optimized molecular structure, the carbons together with germanium lie in a plane, there will be a distinct symmetry separation between the transitions in
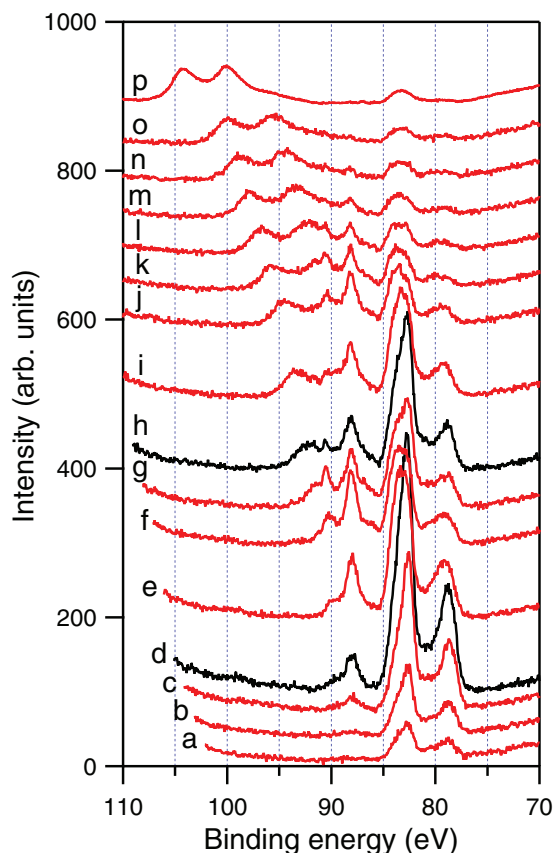


FIG. 2. (Color online) The resonant sCK spectra of $n$-butylgermane measured at the photon energies (in eV and with accuracy of $\pm 0.1$ eV): Spectrum (a) 121.9, (b) 122.9, (c) 123.9, (d) 124.9, (e) 125.9, (f) 126.9, (g) 127.9, (h) 128.9, (i) 129.9, (j) 130.9, (k) 131.9, (l) 132.9, (m) 133.9, (n) 134.9, (o) 135.9, and (p) 139.9.

photoabsorption, a symmetry separation that corresponds to the polarization dependence in the experiment. We present the calculated Ge $3p$ absorption spectra for NBG in Fig. 1(b). We note that the $M_2$ and $M_3$ spectra largely follow the 2:1 rule, i.e., what separates the two spectra is a mere translation of energy due to the spin-orbit splitting and a two-to-one ratio in intensities due to the electron counts. This rule can be expected to hold well only in cases with a sizable spin-orbit coupling, when the channel interaction is small.

Figure 2 shows the resonant sCK decay spectra of NBG measured in the vicinity of the Ge $3p$ edge. The Ge $3d$ lines were by far the most intense features in the measured spectra, but they are located too far away, around 37 eV binding energy, to be displayed. The Ge $3d^{-1}$ states can, in principle, be populated through participator processes from the core-excited states. However, the intensities of the Ge $3d$ photoelectron lines normalized to the photon flux decreased smoothly across the Ge $3p$ resonance region, indicating that the resonant channel to the Ge $3d^{-1}$ states was weak. The intensities of the spectra in Fig. 2 have therefore been scaled so that the Ge $3d$ photoelectron lines have the same heights. The only instrumental factor that could slightly distort the spectral intensities is the transmission of the electron analyzer, which was not determined. However, its effect is expected to be weak at these kinetic energies ($\sim$30–50 eV) and it cannot

in any case explain variations of the peak intensities that occur when the photon energy is only changed by a couple of eVs across a given Ge $3p$ resonance.

Based on the resonant photoemission study of solid Ge at the $3p$ edge [8], the peaks in Fig. 2 can be assigned to resonant sCK transitions $3p^{-1}\text{virt}^1 \rightarrow 3d^{-2}\text{virt}^1$, where virt (for virtual) denotes an electron orbital that is not occupied in the molecular ground state. The use of narrow photon-band excitation (70 meV) practically removes the lifetime broadening of the core-excited $3p^{-1}\text{virt}^1$ states in the measured electron spectra, but the lifetime widths of the $3d^{-2}\text{virt}^1$ final states still broaden the experimental profiles. The energy level structures of $3d^{-2}\text{virt}^1$ states are governed by the two holes in the Ge $3d$ orbitals. The coupling of the $3d^{-2}$ configuration in Ge atoms gives the following LS terms: $^1S_0$, $^1G_4$, $^3P_{0,1,2}$, $^1D_2$, and $^3F_{2,3,4}$ (see, e.g., [27]). The $^1G$ term receives the most intensity in resonant sCK decay of solid Ge, followed by the $^3F$ term [8]. These terms are separated by about 3.9 eV in solid Ge. A similar splitting is observed between the two maxima in the lowermost spectra in Fig. 2, hence we assign them to the $^1G$ and $^3F$ terms. Both of them show asymmetry in the high binding energy side, which is probably due to the excitation of vibrational modes during resonant sCK decay. The intensities of these peaks reach a maximum in spectrum d ($h\nu = 124.9$ eV) and display also a second, lower maximum in spectrum h ($h\nu = 128.9$ eV); these two spectra are displayed in black in Fig. 2. These photon energies agree well with the two maxima in the Ge $3p$ excitation spectrum in Fig. 1(a) and they obviously represent transitions to the most intense states in the calculated $M_3$ and $M_2$ spectra in Fig. 1(b), being associated with electronic excitations to a single virtual orbital we label $R1$. Consequently, the peaks appearing at the binding energies 82.8 and 78.8 eV are assigned to the $3d^{-2}(^1G,^3F)R1^1$ final states.

A new peak emerges at the binding energy of $\sim 88$ eV in spectrum c ($h\nu = 123.9$ eV), reaches a maximum intensity in spectrum f ($h\nu = 126.9$ eV) and a second maximum in spectrum j ($h\nu = 130.9$ eV). These peaks are interpreted to originate from $3p$ excitations to another virtual orbital, which we denote by $R2$. This putative excitation is not resolved in the total ion yield spectrum of Fig. 1(a), but it likely corresponds to the calculated transitions at $\sim 130.8$ eV in Fig. 1(b), which originate from $3p_{3/2}$ excitations to a single virtual orbital. A further decay peak appears in some spectra at the binding energy of $\sim 90.5$ eV. It has the highest intensity at the photon energy of 127.9 eV (spectrum g) and we attribute it to resonant sCK decay following a Ge $3p \rightarrow R3$ excitation. This third resolved excitation is assigned to the peak at 131.3 eV in the calculated $M_3$ spectrum in Fig. 1(b) and, in contrast to the other two identified transitions, this one involves a 85%/15% mixing of two final electronic states. We assume that the relatively sharp peaks between 88 and 92 eV binding energy are caused by the $3d^{-2}(^1G)\text{virt}^1$ states, where virt is $R2$ and $R3$. The $3d^{-2}(^3F)\text{virt}^1$ states for $R2$ and $R3$ are not resolved, but their positions could be pointed out with the help of the known splitting between the $^1G$ and $^3F$ peaks. Finally, the two leftmost features in spectrum p of Fig. 2 are assigned to normal sCK decay of the $3p^{-1}$ states.

According to the above interpretation of resonant sCK spectra, three different virtual orbitals ($R1$–$R3$) are represented in the four most intense peaks. Can we find where the Ge $3p \rightarrow$
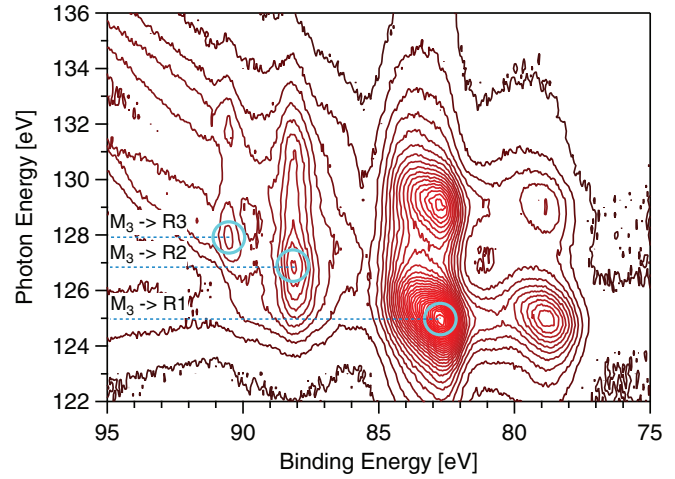


FIG. 3. (Color online) A contour plot of the relative intensities of the resonant sCK spectra measured at the Ge $3p$ edge. The circles denote the intensity maxima of the $3d^{-2}(^1G)\text{virt}^1$ final states resulting from the different Ge $3p_{3/2}$ excitations; the ordinates of the maxima give the excitation energies of the resonances.

$R2, R3$ excitations are located if we follow the intensities of these peaks as a function of photon energy? To find an answer, we remeasured the resonant sCK spectra of NBG at the Ge $3p$ edge using a photon energy step of 0.25 eV. The integrated intensities of these spectra are plotted in Fig. 1(a) after normalization to the photodiode current; the curve is labeled as PEY in Fig. 1 and it represents intensities after the subtraction of a constant background. The decay spectra could be analyzed individually to determine the excitation functions of different final states, but we demonstrate here that the resonances can be visualized simply by drawing a contour plot of the relative intensities, as shown in Fig. 3. The intensities of the spectra for this representation were scaled so that the Ge $3d$ photoelectron lines had the same peak heights, but no other data treatment has been done. Maxima in the contour plot represent the combinations of photon energy (excitation) and binding energy (final states of resonant sCK decay) that enhance intensity.

We can easily identify three maxima that correspond to resonant decay to the $3d^{-2}(^1G)\text{virt}^1$ final states following the Ge $3p_{3/2} \rightarrow R1$–$R3$ excitations; they are evidenced by circles in Fig. 3. The ordinates of the maxima give the excitation energies: Ge $3p_{3/2} \rightarrow R1$ is at $124.97(\pm 0.10)$ eV, Ge $3p_{3/2} \rightarrow R2$ is at $126.8(\pm 0.2)$ eV, and Ge $3p_{3/2} \rightarrow R3$ is at $127.9(\pm 0.3)$ eV. The first value agrees well with the result obtained from the fit of the core excitation spectrum in Fig. 1(a) (124.91 eV). The Ge $3p_{1/2} \rightarrow R1$–$R3$ excitations are almost as visible in Fig. 3; they are located vertically above the circles by the amount of the Ge $3p$ spin-orbit splitting (4.2 eV). The maxima that appear at the binding energy of 78.8 eV are due to the $3p \rightarrow R1$ excitations, but the final states reached are $3d^{-2}(^3F)R1^1$. A close inspection of the $3d^{-2}(^1G,^3F)R1^1$ final states reveals that the contour plots around the maxima are not vertically oriented but skewed. This indicates the presence of another core excitation at a slightly higher excitation energy than those of Ge $3p \rightarrow R1$. Fits of individual decay spectra allow us to estimate that this excitation is located at the photon

energy of 125.8($\pm$0.4) eV in the Ge $M_3$ spectrum. It obviously corresponds to the small peak that the calculation predicts just above the most intense absorption maxima in the $M_3$ excitation spectrum [see Fig. 1(b)].

The measurement of two-dimensional resonant sCK spectra directly revealed the positions of the Ge $3p$ core excitations. The peak structure of resonant sCK decay is expected to be similar in other molecules containing Ge atoms, as the studied transitions involve essentially atomiclike orbitals and the effect of the spectator electron is small. We expect that useful results can be also obtained in other elements, where (s)CK decay of $3p$ hole states is energetically allowed, and in molecules where these elements are included. The method may also be applicable to resonant CK decay of $2s$ hole states in molecules that contain third-row elements such as S and Cl. In all measurements of this kind, one should be aware of the possibility that interference between different electronic states can modify the results; this happens if different overlapping core-excited states can decay to the same final states via shake-up or shake-down transitions. Such decay channels would be visible in Fig. 3 so that more intensity maxima would emerge at (or close to) each horizontal line, indicating the population of the different final states from a given core-excited state. We do not observe any signs of that happening. Thus electronic interference effects are concluded to be weak in the present study.

## V. CONCLUSIONS

In conclusion, the structure of the partially resolved Ge $3p$ core excitation spectrum of $n$-butylgermane could be decomposed further with the aid of two-dimensional resonant decay spectra. The Ge $3p$ excitation spectrum was calculated using the static-exchange (STEX) approach that has been extended to include relativistic effects. The calculated and the experimentally extracted spectral structures are in good agreement with each other. The empirical method to uncover unresolved core excitations is not limited to the studied molecule or to the studied transitions, but we expect that it can be exploited in many systems.

[1] P. Glans, R. E. LaVilla, M. Ohno, S. Svensson, G. Bray, N. Wassdahl, and J. Nordgren, Phys. Rev. A **47**, 1539 (1993).

[2] M. Jurvansuu, A. Kivimäki, and S. Aksela, Phys. Rev. A **64**, 012502 (2001).

[3] G. C. King, M. Tronc, F. H. Read, and R. C. Bradford, J. Phys. B **10**, 2479 (1977).

[4] R. Sankari, A. Kivimäki, M. Huttula, T. Matila, H. Aksela, S. Aksela, M. Coreno, G. Turri, R. Camilloni, M. de Simone, and K. C. Prince, Phys. Rev. A **65**, 042702 (2002).

[5] A. Kivimäki, A. Naves de Brito, S. Aksela, H. Aksela, O.-P. Sairanen, A. Ausmees, S. J. Osborne, L. B. Dantas, and S. Svensson, Phys. Rev. Lett. **71**, 4307 (1993).

[6] D. Anin, K. Jänkälä, S.-M. Huttula, and M. Huttula, Phys. Rev. A **86**, 063410 (2012).

[7] F. Maracci, R. Platania, A. C. De A. E. Souza, and G. G. B. De Souza, Chem. Phys. **133**, 291 (1989).

[8] A. Kivimäki, H. Aksela, S. Aksela, and O.-P. Sairanen, Phys. Rev. B **47**, 4181 (1993).

[9] H.-J. Yang and H.-Y. Tuan, J. Mater. Chem. **22**, 2215 (2012).

[10] E. Sokell, A. A. Wills, D. Ćubrić, F. J. Currell, J. Comer, and P. Hammond, J. Electron Spectrosc. Relat. Phenom. **94**, 107 (1998).

[11] M. K. Odling-Smee, E. Sokell, A. A. Wills, and P. Hammond, J. Phys. B **32**, 2529 (1999).

[12] E. Kukk, A. Wills, N. Berrah, B. Langer, J. D. Bozek, O. Nayadin, M. Alsherhi, A. Farhat, and D. Cubaynes, Phys. Rev. A **57**, R1485 (1998).

[13] E. Sokell, A. A. Wills, M. Wiedenhoeft, X. Feng, D. Rolles, and N. Berrah, J. Phys. B **38**, 1535 (2005).

[14] E. P. Kanter *et al.*, Phys. Rev. Lett. **107**, 233001 (2011).

[15] A. Verweyen, Ph. Wernet, P. Glatzel, B. Sonntag, Ch. Gerth, K. Godehusen, and P. Zimmermann, J. Phys. B **33**, 1563 (2000).

[16] H. Wang, R. F. Fink, M. N. Piancastelli *et al.*, J. Phys. B **34**, 4417 (2001).

[17] K. C. Prince *et al.*, J. Synchrotron Radiat. **5**, 565 (1998).

[18] N. Mårtensson, P. Baltzer, P. A. Brühwiler, J.-O. Forsell, A. Nilsson, A. Stenborg, and B. Wannberg, J. Electron Spectrosc. Relat. Phenom. **70**, 117 (1994).

[19] A. Kivimäki, L. Pfeiffer, H. Aksela, E. Nõmmiste, and S. Aksela, J. Electron Spectrosc. Relat. Phenom. **101–103**, 43 (1999).

[20] DIRAC, a relativistic *ab initio* electronic structure program, Release DIRAC12 (2012), written by H. J. Aa. Jensen, R. Bast, T. Saue, and L. Visscher, with contributions from V. Bakken, K. G. Dyall, S. Dubillard, U. Ekström, E. Eliav, T. Enevoldsen, T. Fleig, O. Fossgaard, A. S. P. Gomes, T. Helgaker, J. K. Lærdahl, Y. S. Lee, J. Henriksson, M. Iliaš, Ch. R. Jacob, S. Knecht, S. Komorovský, O. Kullie, C. V. Larsen, H. S. Nataraj, P. Norman, G. Olejniczak, J. Olsen, Y. C. Park, J. K. Pedersen, M. Pernpointner, K. Ruud, P. Sałek, B. Schimmelpfennig, J. Sikkema, A. J. Thorvaldsen, J. Thyssen, J. van Stralen, S. Villaume, O. Visser, T. Winther, and S. Yamamoto (see http://www.diracprogram.org).

[21] U. Ekström, P. Norman, and V. Carravetta, Phys. Rev. A **73**, 022501 (2006).

[22] S. Villaume, U. Ekström, H. Ottosson, and P. Norman, Phys. Chem. Chem. Phys. **12**, 5596 (2010).

[23] U. Ekström, H. Ottosson, and P. Norman, J. Phys. Chem. C **111**, 13846 (2007).

[24] A. D. Becke, J. Chem. Phys. **98**, 5648 (1993).

[25] T. H. Dunning, Jr., J. Chem. Phys. **90**, 1007 (1989).

[26] J. Henriksson, U. Ekström, and P. Norman, J. Chem. Phys. **124**, 214311 (2006).

[27] J. F. McGilp and P. Weightman, J. Phys. C: Solid State Phys. **9**, 3541 (1976).